Synthesis, X-Ray Structures and Infrared Spectroelectrochemistry of Orthometallated Derivatives of Pyrrolyl Complexes of Iron and Manganese formed by Reaction with $[Os_3(CO)_{10}(MeCN)_2]$ †

Stephen P. Best,[a] **Robin J. H. Clark,**[a] **Antony J. Deeming,***[,a] **Roderick C. S. McQueen,**[a] **Nicholas I. Powell,**[a] **Carola Acuña,**[b] **Alejandro J. Arce***[,b] **and Ysaura De Sanctis**[b]
[a] *Department of Chemistry, University College London, 20 Gordon Street, London WC1H 0AJ, UK*
[b] *Instituto Venezolano de Investigaciones Cientificas, Chemistry Center, Apartado 21827, Caracas 1020-A, Venezuela*

The compound $[Fe(C_4H_4N)(C_5H_5)]$ reacts with $[Os_3(CO)_{10}(MeCN)_2]$ to give the air-stable orthometallated compound $[Os_3H\{(C_4H_3N)Fe(C_5H_5)\}(CO)_{10}]$ **1**, the crystal structure of which has been determined. The Os_3 cluster is linked to the Fe atom by the eight-electron donating C_4H_3N ligand. Cyclic voltammetric studies showed that the cation $\mathbf{1}^+$ is formed reversibly with $E_{\frac{1}{2}}$ of 0.32 V (*vs.* ferrocene–ferrocenium). The IR spectrum of $\mathbf{1}^+$ formed at −25 °C in a spectroelectrochemical cell is closely related to that of **1** indicating that there is no geometric rearrangement on oxidation. The extent of interaction between the cluster and the azaferrocenyl group is estimated by the shift of ν(CO) on oxidation. The shift of 8–14 cm^{-1} to higher energy indicates that, although the electron is removed from the azaferrocenyl group, there is nevertheless a significant change in orbital energies at the cluster on oxidation. Cation $\mathbf{1}^+$ decomposes within 1 min at −25 °C, yielding a number of unidentified carbonyl species. The related orthometallated compound $[Os_3H\{(C_4H_3N)Mn(CO)_3\}(CO)_{10}]$ **2** was correspondingly synthesised and characterised by X-ray diffraction.

This paper describes the synthesis and structures of two related orthometallated products from reactions of $[Os_3(CO)_{10}(MeCN)_2]$ with the η^5-pyrrolyl complexes, azaferrocene [(η-cyclopentadienyl)(η-pyrrol-1-yl)iron] and tricarbonyl(pyrrolyl)manganese. These products are the triosmium clusters $[Os_3H\{(C_4H_3N)Fe(C_5H_5)\}(CO)_{10}]$ **1** and $[Os_3H\{(C_4H_3N)Mn(CO)_3\}(CO)_{10}]$ **2**. The synthetic aspects of this study, already reported preliminarily,[1] came out of our work on the reactions of basic nitrogen heterocycles with $[Os_3(CO)_{12}]$ or $[Os_3(CO)_{10}(MeCN)_2]$. Characteristically these react by co-ordination of the nitrogen atom followed by the transfer of an *ortho*-hydrogen atom from carbon to osmium (Scheme 1). Reactions as in Scheme 1 have been described for pyridines,[2–4] quinolines,[2] diazenes,[2] imidazole,[5] benzimidazole,[5] pyrazole[5] and various substituted forms of these. Different chemistry is observed when the nitrogen atom is not basic, that is when the π electrons are more available for co-ordination to metal centres. For example, pyrrole reacts with C–H cleavage and initially without any nitrogen co-ordination (Scheme 2).[6–8] Compound **3** is very reactive and spontaneously isomerises to **4** for which the X-ray structure has been determined.[8] For this reason compound **3** was only characterised spectroscopically but the *N*-methyl analogue is understandably much more stable and its X-ray structure has been determined.[9]

We have now characterised a range of ligands derived from pyrrole, which adopt various co-ordination modes **A**–**F**. The isomeric ligands in compounds **3** and **4** (see **A** and **B**) both deprotonate to give $[Os_3H(C_4H_3N)(CO)_{10}]^-$ which probably contains the structure **C**. The ligand C_4H_3N has been found in four-electron-donating triply bridging forms as in **D** and **E** and here we describe an eight-electron-donating triply bridging form, as in **F**. The consequences of oxidation of metal atom M′ on the metal atoms M have been examined by IR spectroelectrochemistry.

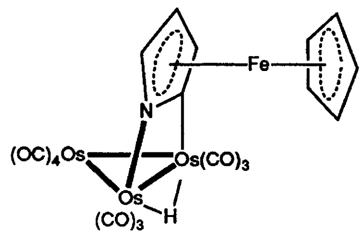

1

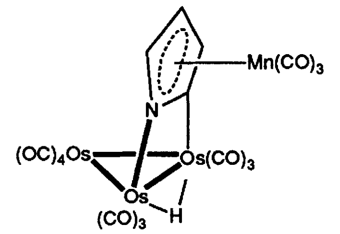

2

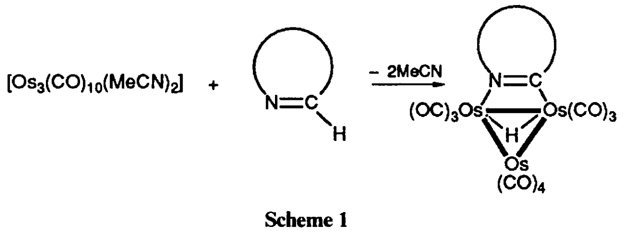

Scheme 1

---

† *Supplementary data available:* see Instructions for Authors, *J. Chem. Soc., Dalton Trans.*, 1991, Issue 1, pp. xviii–xxii.

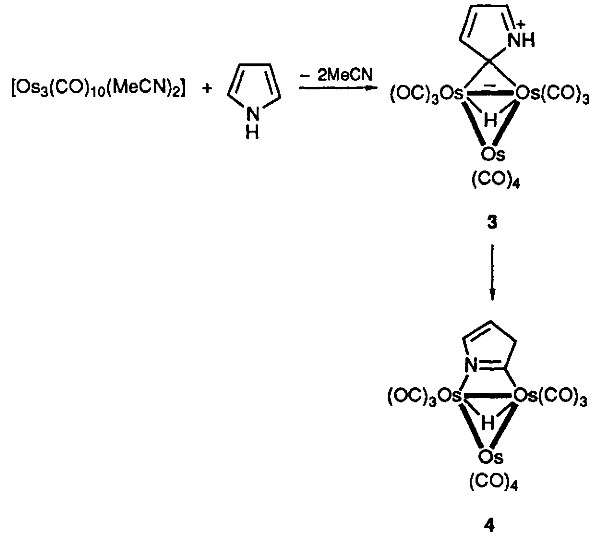

Scheme 2

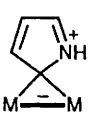

A

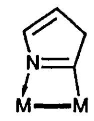

B

C

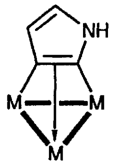

D

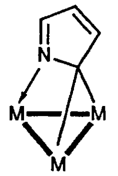

E

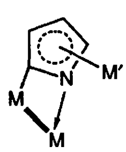

F

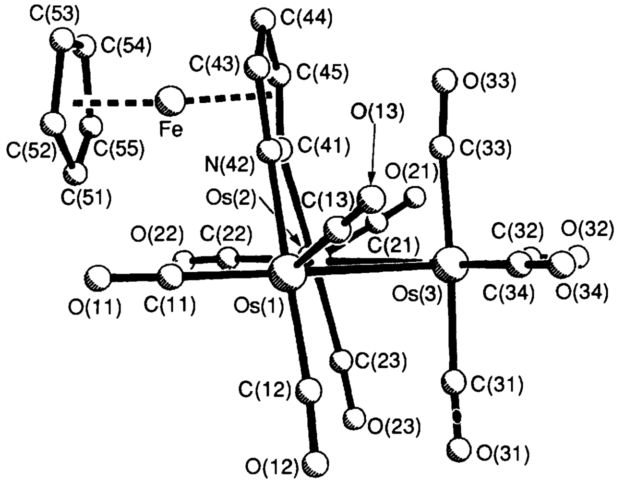

Fig. 1 Molecular structure of $[Os_3(\mu\text{-}H)\{(\mu_3\text{-}C_4H_3N)Fe(C_5H_5)\}(CO)_{10}]$ **1** showing the C(41)N(42) arrangement that is 45% populated. The alternative with C(41) replaced by N(41) and N(42) by C(42) is 55% populated

Results and Discussion

Synthesis and Characterisation.—The cluster $[Os_3(CO)_{10}(MeCN)_2]$ reacts with azaferrocene, $[Fe(C_4H_4N)(C_5H_5)]$, or tricarbonyl(pyrrolyl)manganese, $[Mn(C_4H_4N)(CO)_3]$, in refluxing dichloromethane or cyclohexane, respectively, to give the orthometallated products **1** and **2** as orange crystals in moderate yields.[1] These products were characterised spectroscopically (see Experimental section for data). The ^1H NMR spectra are clearly consistent with orthometallation; signals for a hydride and three pyrrolyl ring protons were observed in each case. The IR spectra around 2000 cm^{-1} were closely similar to those of related products obtained by orthometallation of pyridine, *etc.* (Scheme 1),[2–5] except that the manganese compound **2** also showed three absorptions at 2038, 1964 and 1960 cm^{-1} which are attributed to the *fac*-$Mn(CO)_3$ group. The hydride ^1H NMR shifts were sufficiently different from those of compound **4** (Scheme 2) (δ −13.79 for **1**, −13.98 for **2**, compared with δ −15.10 for **4**) to suggest that the structures might not be directly equivalent so we determined the X-ray crystal structures of **1** and **2**. Their molecular structures are shown in Figs. 1 and 2 and selected bond lengths and angles are in Tables 1 and 2, respectively. The overall structures are as expected and closely related to that of compound **4**.[8] The hydride ligands were not located but the hydride in **1** must bridge the Os(1)–Os(2) edge and lie close to the intersection of the Os(1)–C(13) and Os(2)–C(21) directions and the hydride in **2** is at the corresponding site in that molecule. There is a problem of disorder in both compounds as previously encountered for the imidazolyl compound $[Os_3H(C_3H_3N_2)(CO)_{10}]$ in which the imidazolyl ligand is disordered with some population of each of the two possible orientations of the organic bridge.[5] In compound **2** there is a crystallographic mirror plane passing through Mn and Os(1) and bisecting Os(2) and Os(2a). Hence there must be 50% populations of the pyrrolyl ligand in each of two orientations and we refined the structure in this way. In compound **1** there is no crystallographic requirement of this kind but the disordered populations were allowed to refine and this led to 45 and 55% populations of the forms with different pyrrolyl orientations. This disorder prevented any analysis of the different geometries either in the ligand or at the metal cluster associated with Os–C and Os–N bonds to the pyrrolyl ligands.

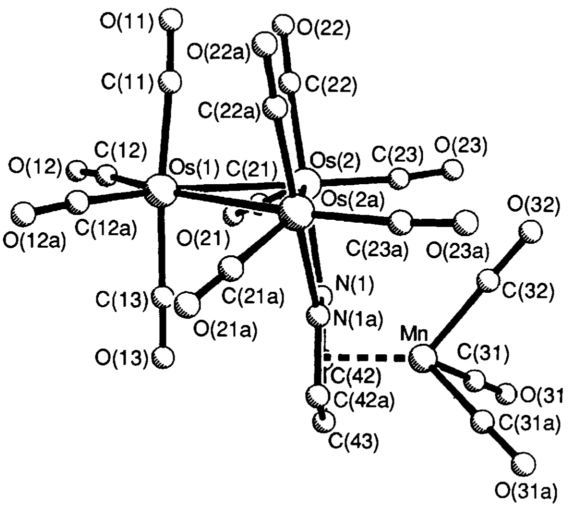

Fig. 2 Molecular structure of $[Os_3(\mu\text{-}H)\{(\mu_3\text{-}C_4H_3N)Mn(CO)_3\}(CO)_{10}]$ **2**. There is a crystallographic mirror plane through the molecule so that N(1), N(1a) and the atoms C(41) and C(41a), that are superimposed on these, are each 50% populated

In both compounds **1** and **2** the pyrrolyl ligands bridge two osmium atoms diaxially while remaining bonded to the Fe and Mn atoms, respectively. The bridged osmium atoms do not lie in the planes of the C_5N rings which are tilted to avoid unfavourable contacts between the $Fe(C_5H_5)$ group and the carbonyls C(11)O(11) and C(22)O(22) in **1** and between the $Mn(CO)_3$ group and the carbonyls C(23)O(23) and its symmetry-related counterpart C(23a)O(23a) in **2**. Thus these distortions move the Fe and Mn atoms away from the hydride ligands and therefore close approaches of this kind do not account for the ^1H NMR hydride shifts as we had, at first, suspected.[1] The $Mn(CO)_3$ group remains co-ordinated to the C_4N ring as in the starting manganese complex and the carbonyl C(32)O(32) lies on the mirror plane. There may well be restricted rotation of the $Mn(CO)_3$ group as a result of the interlocking of the carbonyls C(32)O(32), C(23)O(23) and

Table 1 Selected bond lengths (Å) and angles (°) for $[Os_3H\{(C_4H_3N)Fe(C_5H_5)\}(CO)_{10}]$ **1**

Os(1)–Os(2)	2.938(1)	Os(1)–Os(3)	2.884(1)
Os(2)–Os(3)	2.882(1)	Os(2)–N(41)	2.17(2)
Os(1)–C(42)	2.14(2)	Fe–N(41)	2.05(2)
Fe–C(42)	2.07(2)	Fe–C(43)	2.08(2)
Fe–C(44)	2.05(2)	Fe–C(45)	2.08(2)
Fe–C(51)	2.05(2)	Fe–C(52)	2.08(2)
Fe–C(53)	2.05(2)	Fe–C(54)	2.07(2)
Fe–C(55)	2.08(2)	N(41)–C(42)	1.36(2)
C(42)–C(43)	1.43(2)	C(43)–C(44)	1.43(3)
C(44)–C(45)	1.44(3)	C(45)–N(41)	1.39(2)
C(51)–C(52)	1.40(3)	C(52)–C(53)	1.47(3)
C(53)–C(54)	1.43(3)	C(54)–C(55)	1.44(4)
C(55)–C(51)	1.44(3)		
Os(3)–Os(1)–Os(2)	59.3(1)	Os(3)–Os(2)–Os(1)	59.4(1)
Os(2)–Os(3)–Os(1)	61.3(1)	C(41)–Os(2)–Os(1)	68.3(4)
C(41)–Os(2)–Os(3)	88.6(4)	N(42)–Os(1)–Os(2)	68.5(4)
N(42)–Os(1)–Os(3)	88.0(4)		

Table 2 Selected bond lengths (Å) and angles (°) for $[Os_3H\{(C_4H_3N)Mn(CO)_3\}(CO)_{10}]$ **2**

Os(1)–Os(2)	2.873(1)	Os(2)–Os(2a)	2.965(1)
Os(2)–N(1)	2.11(2)	N(1)–C(41a)	1.46(3)
N(1)–C(42)	1.39(3)	C(42)–C(43)	1.43(3)
Mn–N(1)	2.18(2)	Mn–C(42)	2.18(2)
Mn–C(43)	2.12(3)	Mn–C(31)	1.77(2)
Mn–C(32)	1.83(4)	C(31)–O(31)	1.16(2)
C(32)–O(32)	1.14(4)		
Os–CO	1.89(2) (min.), 1.95(2) (max.), 1.92 (average)		
OsC–O	1.07(3) (min.), 1.14(2) (max.), 1.12 (average)		
N(1)–Os(2)–Os(1)	89.1(4)	N(1)–Os(2)–Os(2a)	69.1(4)
Os–C–O	174(2) (min.), 178.8(8) (max.), 177 (average)		

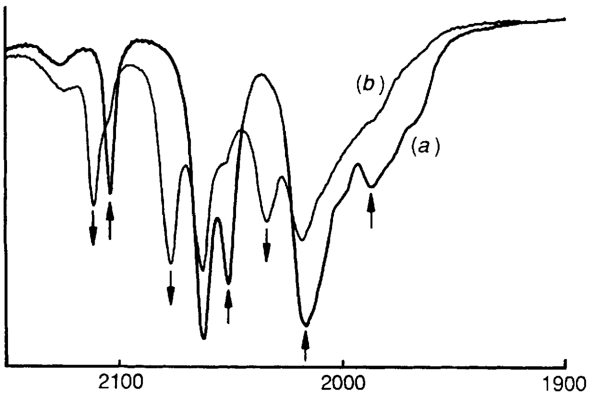

Fig. 3 Infrared spectra in the v(CO) region of compound **1** (*a*) and the oxidised form $\mathbf{1}^+$ (*b*) generated electrochemically in CH_2Cl_2–NBu_4BF_4 at −25 °C. The arrows indicate the changes in intensities on applying an oxidising potential of 1.0 V to a solution of **1**

C(23a)O(23a) but we have neither made sufficient sample of **2** nor of its ^{13}C-enriched form in order to record variable-temperature ^{13}C NMR spectra to establish this point.

Electrochemistry.—Cyclic voltammetry of compound **1** shows that it undergoes a reversible one-electron oxidation ($E_{\frac{1}{2}}$ = 0.32 V) and an irreversible two-electron reduction (E_{pc} = −2.26 V), this having an associated reoxidation at −1.28 V. The oxidation is inferred to be centred on azaferrocene since the oxidation of related clusters without ferrocene or azaferrocene substituents occurs at considerably higher potentials. Azaferrocene itself undergoes an oxidation which is ill defined and irreversible both at room temperature and at −30 °C. Oxidation of the compound by holding the potential at +1.5 V for 3 min and then scanning over the potential range +1.5 to −1.5 V leads to a growth of the current response of the electrode in a manner which suggests the deposition of a polypyrrole film on the surface of the electrode. Such films have been intensively investigated.[10] Evidently the azaferrocene moiety is stabilised in its oxidised form by coupling to the triosmium cluster. It is not clear, at this stage, whether the stabilisation results from steric or electronic considerations.

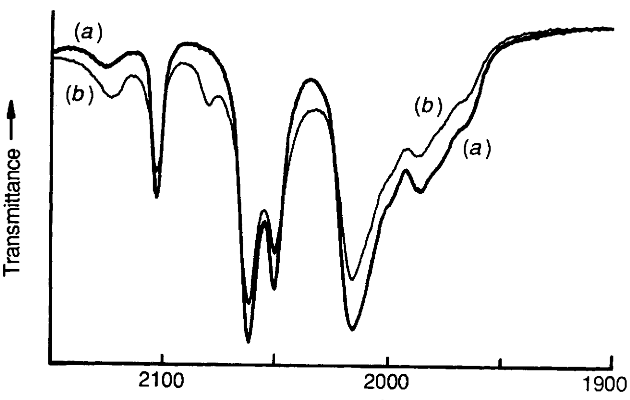

Fig. 4 Infrared spectra of compound **1** in CH_2Cl_2–NBu_4BF_4 at room temperature before oxidation (*a*) and after oxidising electrochemically at −25 °C as in Fig. 3. The oxidising potential was maintained for *ca.* 10 s and then returned to its initial value (*b*)

Spectroelectrochemistry of $[Os_3(\mu\text{-}H)\{(\mu_3\text{-}C_4H_3N)Fe(C_5H_5)\}(CO)_{10}]$ **1**.—The oxidation of cluster **1** in an IR spectroelectrochemical cell leads to collapse of the bands due to v(CO). The oxidation product fails to give a distinct IR spectrum and, on reversing the potential, no recovery of the starting material was observed. Careful examination of the room-temperature spectra failed to reveal the $\mathbf{1}^+$ species whose existence is inferred by the reversibility of the $\mathbf{1}^+$–**1** couple. In order to stabilise the higher concentrations of $\mathbf{1}^+$ produced in the spectroelectrochemical experiment the solution in contact with the working electrode was cooled to −25 °C. Under these conditions a satisfactory spectrum of $\mathbf{1}^+$ was recorded (Fig. 3) although, because of its reactivity ($t_{\frac{1}{2}}$ *ca.* 20 s), it was impossible to eliminate some decompositon. By careful control of the experimental conditions it was possible to regenerate *ca.* 80% of **1** after reoxidation; the appearance of new features in the spectrum indicated that a product was being formed (Fig. 4). The spectrum of $\mathbf{1}^+$ is similar in form, but shifted in wavenumber, to that of **1**. The shift is 8–14 cm^{-1}, about 20% of that expected for a cluster-based oxidation (see ref. 11 and refs. therein). This is in keeping with the oxidation being based on the azaferrocene moiety and that the interaction between azaferrocene and the triosmium cluster is little changed on oxidation. Oxidation of a ferrocene group attached to a triosmium cluster through a μ-acyl group in $[Os_3(\mu\text{-}H)\{COC_5H_4Fe(C_5H_5)\}(CO)_{10}]$ also gives a shift to higher wavenumbers in v(CO) (by 6–8 cm^{-1}), *i.e.* less than that found for the more directly linked azaferrocene cluster.[11] Comparison of the spectra of the clusters in their neutral and one-electron oxidised forms shows that the spectra are most similar in the oxidised state, indicating that ferrocene and azaferrocene are more similar in terms of their interaction with the triosmium cluster in their oxidised forms. Studies of a series of ferrocene tricobalt carbonyl clusters, $[Co_3\{\mu_3\text{-}C(C_5H_4)Fe(C_5H_5)\}(CO)_{9-n}L_n]$ [n = 0–3, L = PPh_3 or $P(OPh)_3$], have shown that the sensitivity of v(CO) to ferrocene oxidation depends upon the richness of the cluster with shifts of between 12 (n = 0) and 23 cm^{-1} [n = 3, L = $P(OPh)_3$].[12] While the structures of the

Table 3 Crystallographic data for compounds **1** and **2**

	1	**2**
Formula	$C_{19}H_9FeNO_{10}Os_3$	$C_{17}H_4MnNO_{13}Os_3$
M	1037.74	1055.76
Crystal size/mm	0.30 × 0.20 × 0.07	0.50 × 0.10 × 0.24
Crystal system	Monoclinic	Orthorhombic
Space group	$P2_1/c$	*Pcmn*
a/Å	14.376(5)	11.113(2)
b/Å	11.286(2)	13.930(3)
c/Å	14.499(3)	14.840(2)
β/°	100.77(2)	90
U/Å^3	2311(1)	2297(1)
Z	4	4
D_c/g cm^{-3}	2.98	3.05
μ(Mo-Kα)/cm^{-1}	171.3	171.4
F(000)	1856	1880
2θ range/°	5–50	5–50
No. unique data	4087	2122
Rejection criterion	$F_o < 5\sigma(F_o)$	$F_o < 3\sigma(F_o)$
No. reflections used	3462	1775
Parameters refined	298	155
R^a	0.0601	0.0637
R'^b	0.0572	0.0622
g in weighting scheme	0.006 96	0.000 738
Max. shift/e.s.d. in final refinement	0.571	0.001
Largest residual peak (close to Os)/e Å^{-3}	3.4	3.1

^{a} $R = \Sigma[|F_o| - |F_c|]/\Sigma|F_o|$. ^{b} $R' = [\Sigma w(|F_o| - |F_c|)^2/\Sigma w|F_o|^2]^{\frac{1}{2}}$, $w = [\sigma^2(F_o) + g(F_o{}^2)]^{-1}$.

Table 4 Fractional atomic coordinates (× 10^4) for compound **1**

Atom	x	y	z
Os(1)	2983(1)	207(1)	8440(1)
Os(2)	2627(1)	380(1)	6382(1)
Os(3)	1261(1)	1263(1)	7437(1)
Fe	3243(2)	−2790(2)	7277(2)
C(41)	2358(11)	−1392(13)	6847(10)
N(42)	2506(11)	−1442(14)	7797(10)
C(43)	2191(13)	−2565(14)	8068(13)
C(44)	1842(13)	−3192(18)	7214(15)
C(45)	1936(14)	−2424(15)	6441(16)
C(51)	4662(14)	−2499(18)	7340(17)
C(52)	4548(14)	−3229(19)	8094(17)
C(53)	4016(17)	−4279(18)	7699(19)
C(54)	3872(15)	−4189(20)	6700(18)
C(55)	4279(19)	−3085(25)	6471(18)
O(11)	4816(10)	−971(12)	9348(10)
C(11)	4134(13)	−521(16)	8997(12)
O(12)	3694(12)	2648(14)	9158(12)
C(12)	3392(14)	1758(17)	8860(12)
C(21)	1658(18)	371(19)	5316(15)
O(21)	1020(14)	338(17)	4649(11)
C(22)	3577(16)	−236(19)	5735(13)
O(22)	4122(14)	−507(15)	5313(14)
O(23)	3111(14)	2946(13)	6016(12)
C(23)	2919(15)	2024(17)	6144(14)
O(32)	−297(13)	2249(17)	5888(11)
O(31)	2189(15)	3717(14)	7636(15)
C(32)	301(13)	1859(16)	6473(13)
C(31)	1878(15)	2807(17)	7578(13)
O(33)	309(11)	−1168(13)	7188(12)
O(13)	1881(11)	−262(14)	9991(10)
O(34)	391(14)	1709(18)	9154(11)
C(33)	704(14)	−326(16)	7277(13)
C(13)	2305(15)	−82(18)	9443(12)
C(34)	697(19)	1550(19)	8520(14)

Table 5 Fractional atomic coordinates (× 10^4) for compound **2**

Atom	x	y	z
Os(1)	863(1)	7500	6488(1)
Os(2)	2595(1)	6436(1)	5455(1)
Mn	5770(3)	7500	5975(3)
C(41)	3969(13)	6977(11)	6297(10)
N(1)	3969(13)	6977(11)	6297(10)
C(42)	4759(19)	6661(15)	6961(13)
C(43)	5289(25)	7500	7356(19)
C(11)	−146(22)	7500	5415(17)
O(11)	−760(20)	7500	4858(15)
C(12)	17(20)	6439(14)	7013(13)
O(12)	−432(15)	5798(12)	7348(11)
C(13)	2004(24)	7500	7470(19)
O(13)	2663(20)	7500	8042(13)
C(21)	2326(15)	5355(13)	6207(11)
O(21)	2155(18)	4720(12)	6667(12)
C(22)	1299(16)	6058(13)	4656(12)
O(22)	596(16)	5812(11)	4189(12)
C(23)	3766(17)	5865(13)	4700(14)
O(23)	4397(15)	5492(11)	4204(11)
C(31)	6890(17)	6598(13)	5919(17)
O(31)	7609(13)	5999(13)	5888(15)
O(32)	5648(23)	7500	3979(14)
C(32)	5677(28)	7500	4746(24)

cobalt and osmium clusters are markedly different the effect of oxidising the parent clusters is similar in both cases.

Experimental

Syntheses.—$[Os_3H\{(C_4H_3N)Fe(C_5H_5)\}(CO)_{10}]$ **1**. A solution of $[Os_3(CO)_{10}(MeCN)_2]$ (0.103 g, 0.108 mmol) and azaferrocene (0.058 g, 0.310 mmol) in dichloromethane (30 cm^3) was heated under reflux for 2 h by which time the IR spectrum showed that the reaction was complete. Attempted separation by TLC on silica led to very extensive decomposition to $[Os_3H(C_4H_4N)(CO)_{10}]$ **3** which was always obtained as a by-product in varying amounts. The best work-up was to add Florosil to the crude dichloromethane solution and to evaporate to dryness. The dry Florosil was added to the top of a Florosil column (diameter 2.5 cm) which was eluted with light petroleum (b.p. 40–60 °C) to give an orange band containing pure product. Yields of similar reactions were 37 (0.041) to 61% (0.068 g), the higher yields being for shorter contact times with Florosil. IR (cyclohexane): ν(CO)/cm^{-1} 2103m, 2061vs, 2051s, 2020vs, 2011s, 2001m, 1982m and 1972w. ^{1}H NMR (CDCl$_3$): δ 5.76 (br, H^x), 4.64 (dd, H^y), 4.50 (dd, H^z), 4.30 (s, C$_5$H$_5$) and

-13.79 (s, OsH), $J(H^xH^y)$ not clearly measurable, $J(H^xH^z)$ 1.1, $J(H^yH^z)$ 2.5 Hz. Evaporation of a hexane solution gave air-stable orange crystals suitable for X-ray crystallography.

$[Os_3H\{(C_4H_3N)Mn(CO)_3\}(CO)_{10}]$ **2**. A mixture of $[Os_3(CO)_{10}(MeCN)_2]$ (0.101 g, 0.106 mmol) and $[Mn(C_4H_4N)(CO)_3]$ (0.046 g, 0.224 mmol) in cyclohexane (70 cm^3) was heated under reflux for 5 h. The product was more stable than **1** towards silica and TLC [SiO_2, eluent light petroleum (b.p. 40–60 °C)] gave one main orange band which yielded orange-red crystals of compound **2** (0.031 g, 28%). IR (cyclohexane): ν(CO)/cm^{-1} 2107m, 2068vs, 2059vs, 2025vs, 2009vs, 1997m, 1981m [$Os_3(CO)_{10}$ group], 2038m, 1964m, 1960m [$Mn(CO)_3$ group]. ^{1}H NMR ($CDCl_3$): δ 6.40 (br, H^x), 5.20 (dd, H^y), 4.70 (dd, H^z) and -13.98 (s, OsH), $J(H^xH^y)$ 0.7, $J(H^xH^z)$ 1.5 and $J(H^yH^z)$ 2.6 Hz. Crystals suitable for crystallography were obtained by evaporation of hexane solutions.

Crystal-structure Determinations for Compounds **1** *and* **2**.—Crystals of compounds **1** and **2** were grown by evaporation of hexane solutions. General crystallographic data and structure determination parameters are in Table 3 and atomic coordinates of **1** and **2** are in Tables 4 and 5 respectively. Crystals of each were mounted on a Nicolet R3v/m diffractometer and centred using orientation reflections obtained from a rotation photograph. Intensity data were collected at room temperature using graphite-monochromated Mo-Kα radiation ($\lambda = 0.71073$ Å) using the ω–2θ scan method. Reflection intensities were corrected for Lorentz and polarisation effects and for decay by fitting data to a curve calculated from three standard reflections collected regularly throughout the data collection; the extent of decay was 4 and 6% for compounds **1** and **2** respectively. Absorption corrections were made by the azimuthal scan method; maximum and minimum transmission factors are 1.000 and 0.248 for **1** and 1.000 and 0.111 for **2**. The structures were solved by routine application of direct methods and refined by alternating cycles of full-matrix least squares and by Fourier difference synthesis. All calculations were carried out on a MicroVax II computer using SHELXTL PLUS.[13]

Disorder in compound **1** involved the arrangement shown in Fig. 1 disordered with another with the osmium-bonded atoms C(41) and N(42) reversed, labelled N(41) and C(42) in this reversed arrangement. The best refinement gave C(41)N(42) with 45% population and N(41)C(42) with 55% population. These populations were fixed in the final refinement with isotropic thermal parameters of C(41) and C(42) fixed as equal and allowed to refine and with atoms N(41) and N(42) treated likewise. All other atoms in **1** were refined anisotropically. Since there is a crystallographic mirror plane through molecules of **2**, the disorder of osmium-bonded C and N atoms was necessarily 50% each. All non-H atoms in **2** were refined anisotropically except C(12), which could not be refined anisotropically so was left isotropic, and the atoms of the organic ring. No hydrogen atoms were included in the models of compound **1** or **2**.

Additional material available from the Cambridge Crystallographic Data Centre comprises thermal parameters and remaining bond lengths and angles.

Electrochemistry of Compound **1**.—Experiments were carried out using a Metrohm E506 potentiostat and an E506 VA scanner. Platinum wires were used as working and counter electrodes for voltammetric experiments, while the reference electrode was Ag–AgCl (Metrohm EA441/5); all potentials are quoted with respect to the ferrocene–ferrocenium couple. Dichloromethane, distilled from P_2O_5, was used as solvent with tetra-n-butylammonium tetrafluoroborate as supporting electrolyte.

Spectroelectrochemistry.—Infrared spectra were recorded using a Bruker IFS 113V Fourier-transform interferometer utilising a Ge-coated KBr beamsplitter and a liquid-nitrogen-cooled MCT detector. The spectroelectrochemical cell has been described elsewhere.[14]

Acknowledgements

We thank Miss S. A. Ciniawskii for running the electrochemical experiment on azaferrocene. We also thank the SERC for a studentship (for N. I. P.) and a fellowship (for R. C. S. McQ.), for support for a diffractometer, and for other support and the University of London Intercollegiate Research Service (ULIRS) for use of the FTIR spectrometer.

References

1 A. J. Arce, C. Acuña and A. J. Deeming, *J. Organomet. Chem.*, 1988, **356**, C47.
2 C. Choo Yin and A. J. Deeming, *J. Chem. Soc., Dalton Trans.*, 1975, 2091; A. J. Deeming, R. Peters, M. B. Hursthouse and J. D. J. Backer-Dirks, *J. Chem. Soc., Dalton Trans.*, 1982, 787.
3 B. F. G. Johnson, J. Lewis and D. A. Pippard, *J. Organomet. Chem.*, 1978, **145**, C4.
4 A. D. Clauss, J. R. Shapley and S. R. Wilson, *J. Am. Chem. Soc.*, 1981, **103**, 7387.
5 J. R. Shapley, D. E. Samkoff, C. Bueno and M. R. Churchill, *Inorg. Chem.*, 1982, **21**, 634; M. R. Churchill and J. R. Missert, *J. Organomet. Chem.*, 1983, **256**, 349.
6 A. J. Arce, Y. De Sanctis and A. J. Deeming, *J. Organomet. Chem.*, 1986, **311**, 371.
7 A. J. Deeming, A. J. Arce, Y. De Sanctis, M. W. Day and K. I. Hardcastle, *Organometallics*, 1989, **8**, 1408.
8 M. W. Day, K. I. Hardcastle, A. J. Deeming, A. J. Arce and Y. De Sanctis, *Organometallics*, 1990, **112**, 6.
9 A. J. Deeming, A. J. Arce and Y. De Sanctis, unpublished work.
10 A. F. Diaz, K. K. Kanazawa, J. I. Castillo and J. A. Logan, in *Conductive Polymers*, ed. R. V. Seymour, Plenum, New York, 1981, p. 149 and refs. therein; A. F. Diaz and J. Bargon, in *Handbook of Conducting Polymers*, ed. T. A. Skotheim, Marcel Dekker, New York, 1986, p. 81; C. B. Street, in *Handbook of Conducting Polymers*, ed. T.A. Skotheim, Marcel Dekker, New York, 1986, p. 265 and refs. therein.
11 A. J. Arce, P. A. Bates, S. P. Best, R. J. H. Clark, A. J. Deeming, M. B. Hursthouse, R. C. S. McQueen and N. I. Powell, *J. Chem. Soc., Chem. Commun.*, 1988, 478.
12 S. Colbran, B. H. Robinson and J. Simpson, *J. Chem. Soc., Chem. Commun.*, 1982, 1361; *Organometallics*, 1983, **2**, 952.
13 G. M. Sheldrick, SHELXTL PLUS, An integrated system for refining and displaying crystal structures from diffraction data, University of Göttingen, 1986.
14 S. P. Best, R. J. H. Clark, R. P. Cooney and R. C. S. McQueen, *Rev. Sci. Instrum.*, 1988, 58, 2071.

Received 21*st August* 1990; *Paper* 0/03836I